PETROGENESIS AND SHOCK METAMORPHISM OF THE NEWLY-FOUND BASALTIC LUNAR METEORITE NORTHWEST AFRICA 14526: PRELIMINARY RESULTS. Tian-Ran T. Du[1], and Ai-Cheng Zhang[1]. [1]School of Earth Sciences and Engineering, Nanjing University, Nanjing 210023, China, E-mail: trindu@foxmail.com.

Introduction: Lunar basalts have formed through partial melting of lunar mantle. They are critical samples for constraining the volcanic history of the Moon and the evolution of the lunar mantle [1,2]. Investigations of lunar basalts collected by Apollo, Luna, and Chang'e missions have constructed a framework for the lunar volcanic history. For example, the major volcanism on the Moon took place from 3.85 to 3.0 Ga, although lunar volcanism can be prolonged to approximately 2.0 Ga [3]. Basaltic lunar meteorites have provided complementary materials to understand lunar volcanism, especially they are probably derived from source regions that have not been sampled by previous sample-return missions. Although over 580 lunar meteorites have been identified, the number of basaltic lunar meteorites is rather limited. Northwest Africa (NWA) 14526 is a newly-found unbrecciated basaltic lunar meteorite [4]. We are performing petrologic and geochronological study on this meteorite in order to understand its petrogenesis and potential implications to the lunar volcanism. Here, we report the preliminary results of our petrographic and mineralogical observations on this meteorite.

Methods: Petrographic observations were conducted with a Zeiss Supra 55 field emission scanning electron microscope. An electron probe microanalyzer was used to measure chemical compositions of rock-forming minerals. Structural characterization of minerals was performed with a Renishaw RM2000 Laser Raman Microscope.

Results: NWA 14526 is a lunar basalt meteorite with coarse-grained anti-ophitic to gabbroic texture (Fig. 1). Three polished sections have been used for petrographic observations. The modal abundances of rock-forming minerals are 14.3 vol% olivine, 52.8 vol% pyroxene, 29.0 vol% plagioclase, and 2.1 vol% ilmenite. X-ray elemental mapping results show that NWA 14526 contains two different regions (Fig. 1), which have distinctly different modal abundances in plagioclase. We term them Pl-rich region and Pl-poor region, respectively. Chromite grains exclusively occur in the Pl-rich region. Ilmenite, silica phases, K-feldspar, Fe-sulfide, Ca-phosphate, baddeleyite, and zirconolite mainly occur in the Pl-poor region. Ulvöspinel grains occur in both regions. The Pl-poor region appears as veins cutting through the Pl-rich region (Fig. 1); however, the boundary between these two regions is vague.

The Pl-rich region has an anti-ophitic texture, with the space between subhedral-euhedral olivine and pyroxene grains filled by anhedral plagioclase grains. Most olivine grains in this region are zoned in BSE images. Pyroxene grains in the Pl-rich region vary in size from 0.2 to 1 mm. Most of them show complex compositional zonation, with pigeonite cores, augite mantles, and pigeonite rims. Thin exsolution lamellae (usually submicron but up to 3 μm in width) are ubiquitous in most pyroxene grains. Chromite and ulvöspinel usually occur as subhedral-euhedral inclusions (10–500 μm in length) in pyroxene, plagioclase, and olivine. Some chromite grains are zoned while some ulvöspinel grains contain ilmenite lamellae.

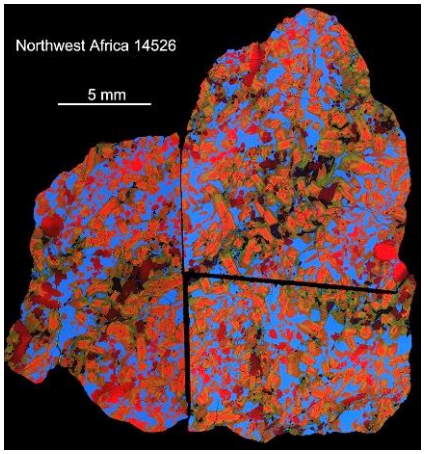

Fig. 1. The false-color image of X-ray elemental mapping (Mg-red, Ca-green, Al-blue) results of NWA 14526.

The Pl-poor region is mainly composed of pyroxene, olivine, and ilmenite, with minor other phases. Olivine in this region is usually anhedral to euhedral and 0.1–1 mm in length. Most olivine grains contain ulvöspinel inclusions, and some contain inclusions of quartz, K-feldspar, and ilmenite. Pyroxene grains in this region are larger (0.5–2 mm) compared with those in the Pl-rich region and also show complex zonation. As shown in Fig. 1, pyroxene grains in the Pl-poor region have greener rims, which are Ca-rich but Mg-poor. Ilmenite grains are subhedral to anhedral and 0.1–1 mm in length. Some ilmenite grains contain melt inclusions. Ulvöspinel in the Pl-poor region also contains ilmenite lamellae. Silica phase, K-feldspar, zirconolite, baddeleyite, merrillite, apatite, and minor pigeonite are present together in the

interstitial regions between coarse-grained minerals in the Pl-poor region. Quartz usually forms intergrowths with K-feldspar. Fine-grained symplectites of hedenbergite + fayalite + SiO_2 are also observed in the Pl-poor region.

Minerals in NWA 14526 are highly fractured. Plagioclase has partially transformed into maskelynite. Shock-induced melt veins, which are relatively thin (5–100 μm in width), are commonly observed in NWA 14526. They are composed of glass, fine-grained minerals, and some relict fragments. Tissintite occurs as fine-grained aggregates at the edge of the glassy melt veins or comprises the majority of some melt veins in plagioclase. Olivine grains adjacent to melt veins have partially transformed into ringwoodite. We also observed stishovite and seifertite in the Pl-poor region. Seifertite usually shows a tweed-like texture while stishovite appears as clustered fibers.

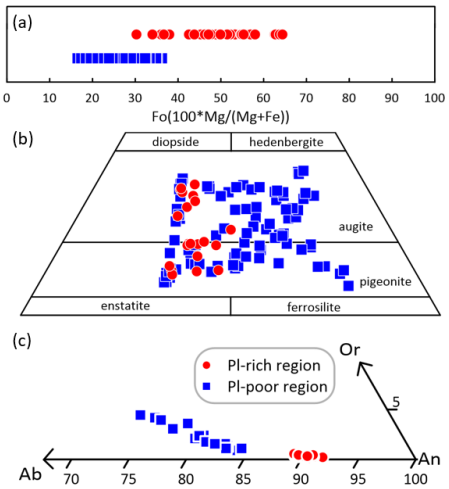

Fig. 2. Chemical compositions of olivine, plagioclase, and pyroxene in NWA 14526.

Chemical compositions of rock-forming minerals in both Pl-rich and Pl-poor regions are illustrated in Fig. 2. Olivine shows a large compositional variation ($Fo_{16.5–64.5}$), but those in the Pl-poor region are generally Fe-enriched than those in the Pl-rich region. The pyroxene grains in the Pl-poor region show a large compositional range ($En_{12.8–60.8}Fs_{20.3–74.1}Wo_{8.0–39.2}$, Mg#=19.2–68.7) than those in the Pl-rich region ($En_{38.2–57.8}Fs_{20.8–38.3}Wo_{11.1–35.8}$, Mg#=49.9–68.1; Fig. 2b). The compositions of pigeonite grains associated with silica and K-feldspar are $En_{12.8–24.1}Fs_{44.0–74.1}Wo_{8.0–39.5}$ (Mg#=19.2–33.2). The correlation between Ti/(Ti+Cr) and Fe/(Fe+Mg) is consistent with the trend for low-Ti mare basalts, but different from the trends for high-Ti and very low-Ti mare basalts (Fig. 3). Plagioclase grains in the Pl-poor region have much higher Ab and Or values than those in the Pl-rich region (Fig. 2c).

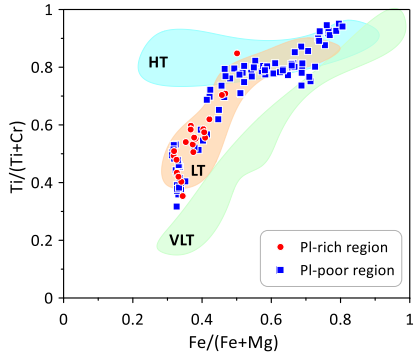

Fig. 3. Ti/(Ti+Cr) versus Fe/(Fe+Mg) of pyroxene in NWA 14526. Fields [5] of high-Ti (HT), low-Ti (LT), and very low-Ti (VLT) are shown for comparison.

Discussion and Conclusion: The correlation between Ti/(Ti+Cr) and Fe/(Fe+Mg) of pyroxene shown in Fig. 3 indicates that NWA 14526 is a low-Ti lunar basalt, which is consistent with the suggestion based on the compositions of quenched melt veins [4].

Our petrographic observations show that NWA 14526 contains two different regions, Pl-rich and Pl-poor regions. The Pl-rich region only consists of olivine, pyroxene, anorthite, chromite, and ulvöspinel; however, the Pl-poor region contains ilmenite, silica, K-feldspar, Zr-minerals, and Ca-phosphate minerals, besides of olivine, pyroxene, plagioclase, and ulvöspinel. This difference indicates that these two regions formed at different stages, and the Pl-rich region should have formed earlier than the Pl-poor region. Chemically, olivine and pyroxene are more Fe-enriched and plagioclase contains more Na and K in the Pl-poor region compared with those in the Pl-rich region. These compositional differences also support the sequence that the Pl-rich region should have formed earlier than the Pl-poor region.

The high-pressure minerals in NWA 14526 probably formed with different mechanisms, e.g., crystallization from HP melts (tissintite and stishovite) and solid-state transformation (ringwoodite and seifertite). The presence of seifertite implies the shock pressure that NWA 14526 experienced could be high up to 40 GPa [6].

Acknowledgements: This work was supported by research grants from NSFC (42025302).

References: [1] Papike J. J. and Vaniman D. T. (1978) *GRL, 5*, 433–436. [2] Papike J. J. et al. (1998) *RM, 7*, 1–11. [3] Li Q. L. et al. (2021) *Nature, 600*, 54–58. [4] Gattacceca J. et al. (2022) *MPS*, 1–4. [5] Robinson K. L. et al. (2012) *MPS, 37*, 387–399. [6] Miyahara M. et al. (2013) *Nat. Commun. 4*, 1737.